



<b>Project:</b>	nanoCOPS
<b>Project Number:</b>	FP7-ICT-2013-11/619166
<b>Work Package:</b>	WP1 Time-domain Simulation of Coupled Problems
<b>Tasks</b>	T1.1: Coupled EM-Device-Circuit and coupled EM-Heat Simulation T1.7: Implementation
<b>Deliverable</b>	D1.3: Integrated circuit-device simulation tool (software library) – Version 2
<b>Scheduled</b>	M18 (April 2015)

<b>Title</b>	D1.3: Integrated circuit-device simulation tool (software library) – Version 2
<b>Authors</b>	The Non-Linear Interface & Implementation Details Christian Strohm, Caren Tischendorf (HUB) Peter Meuris, Wim Schoenmaker (MAG)
<b>Affiliations</b>	Kai Bittner, Hans-Georg Brachtendorf (FHO) HUB: Humboldt University Berlin MAG: MAGWEL NV, Leuven FHO: FH OÖ Forschungs & Entwicklungs GmbH, Hagenberg im Mühlkreis
<b>Contact:</b>	Wim.Schoenmaker@magwel.com
<b>Date</b>	April 18, 2015(M18)

# D1.3: Integrated circuit-device simulation tool (software library)

## Version 2

### The Non-Linear Interface & Implementation Details

Christian Strohm, Caren Tischendorf (HUB),  
Peter Meuris, Wim Schoenmaker (MAG),  
Kai Bittner, Hans-Georg Brachtendorf (FHO)

#### Contents

<b>1</b>	<b>Abstract</b>	<b>3</b>
<b>2</b>	<b>Introduction</b>	<b>4</b>
2.1	Coupled Circuit-Device Simulation . . . . .	4
<b>3</b>	<b>Nonlinear Coupling</b>	<b>6</b>
3.1	MNA . . . . .	6
3.2	EM System . . . . .	6
3.3	Current-continuity equation discretization in metals . . . . .	8
3.4	Current-continuity in semiconductors . . . . .	8
3.5	Gauss' law . . . . .	10
3.6	Maxwell-Ampere law . . . . .	11
3.7	Coupled system . . . . .	11
3.8	Technical realization . . . . .	12
<b>4</b>	<b>Constructing the output vector <math>\mathbf{Y}</math></b>	<b>14</b>
<b>5</b>	<b>Testing the non-linear interface</b>	<b>16</b>
5.1	Testing the Jacobian $J$ . . . . .	16
5.2	Scaling choices . . . . .	19
5.3	Number inspection of the Jacobian . . . . .	22
5.4	Number inspection of $\tilde{A}$ , $\hat{A}$ , $\tilde{b}$ and $\hat{b}$ . . . . .	26
<b>6</b>	<b>Testing the NLI for semiconductors</b>	<b>27</b>
<b>7</b>	<b>Conclusion</b>	<b>34</b>

# 1 Abstract

This report elaborates on technical issues for building the python MECS-Sframe-MAGWEL interface. Specific attention is paid to debugging and testing the non-linear interface.

## 2 Introduction

In this document we present the interface set up of the MAGWEL and MECS solvers. There are two versions of the coupling. In the first version, the interface is based on frequency analysis. It exploits the linearity of materials with respect to variations applied biases. As a consequence, this interface is only applicable if the material response is linear which is the case for simple conductors and insulators. This interface was developed in the ICESTARS project and will be used here mainly for testing the non-linear extension.

### 2.1 Coupled Circuit-Device Simulation

For the first fully coupled simulation with an direct, pointer based, communication between the MAGWEL solver for the electromagnetic field simulation and MECS/Sframe for the circuit equations we consider a semi-closed loop of metal with two contacts, 144 metal nodes, 40 insulator nodes and 188 links as electromagnetic device, see Fig. 1. The circuit contains just two elements namely a simple sinusoidal source connected with the electromagnetic device model. The netlist reads

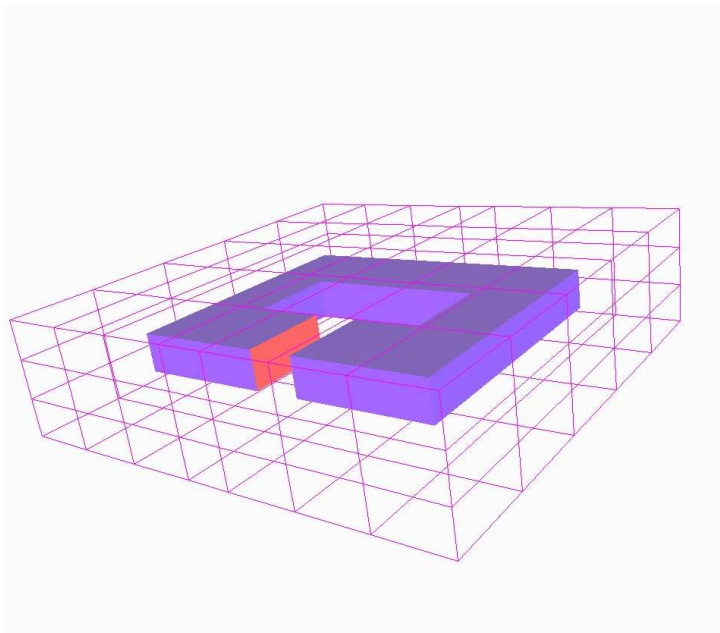


Figure 1: Current through the semi-closed loop

```
* Simple Circuit with one EM-Element, one voltage source and a resistor
V1 1 0 sin(0 1 1 0 0)
$EM1 1 0 simple_test.xml 1
```

where the \$ implies a non-conform Spice3 element, see <http://bwrc.eecs.berkeley.edu/classes/icbook/spice/>. In more detail the line

```
$EM1 1 0 simple_test.xml 1
```

implies that the electromagnetic device is located between node 1 and 0, and is modeled by the MAGWEL xml structure `simple_test.xml` and the 1 say which contact is the

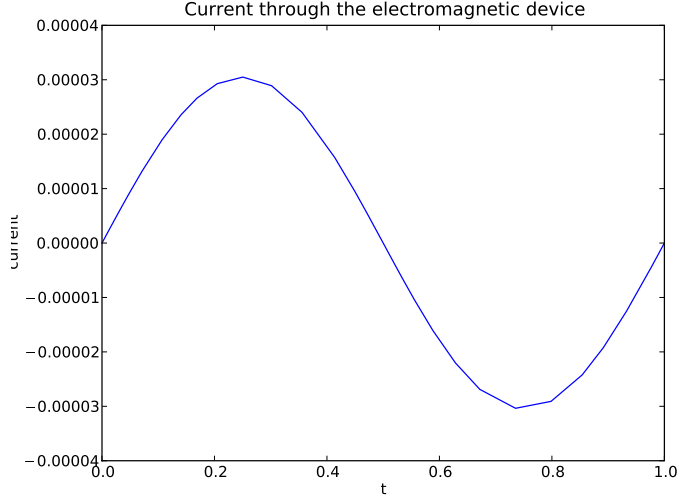


Figure 2: Current through the semi-closed loop

reference contact for the current calculation. Fig. 2 shows the current through the electromagnetic device. DAEn was used to solve the resulting differential-algebraic equation with the standard options.

In general the equations for the coupled circuit-device simulation reads

$$\begin{aligned}
A_C q' + A_{RG}(A_R^T e, t) + A_L j_L + A_M j_M + A_V j_V + A_I i_s(t) &= 0 \\
q - q(A_C^T e, t) &= 0 \\
\phi' - A_L^T e &= 0 \\
\phi - \phi(j_L, t) &= 0 \\
A_V^T e - v_s(t) &= 0 \\
A_{00}\mathcal{V} + A_{10}\frac{d}{dt}\mathcal{V} + A_{11}\Pi + A_{21}\frac{d}{dt}\Pi + B_{00}hA_M^T e + B_{10}hA_M^T \frac{d}{dt}e &= 0 \\
\Pi - \frac{d}{dt}\mathcal{A} &= 0 \\
A_{02}\mathcal{V} + A_{03}\mathcal{A} + A_{12}\frac{d}{dt}\mathcal{V} + A_{13}\Pi + A_{23}\frac{d}{dt}\Pi + B_{01}hA_M^T e + B_{11}hA_M^T \frac{d}{dt}e &= 0 \\
C_{00}\mathcal{V} + C_{10}\frac{d}{dt}\mathcal{V} + C_{11}\Pi + C_{21}\frac{d}{dt}\Pi + D_0hA_M^T e + D_1hA_M^T \frac{d}{dt}e + Lj_M &= 0
\end{aligned}$$

with solution  $x = (e, \phi, j_L, q, j_V, \mathcal{V}, \mathcal{A}, \Pi, j_M)$  and

$$A_i = \begin{bmatrix} A_{i0} & A_{i1} \\ A_{i2} & A_{i3} \end{bmatrix}, C_i = [C_{i0} \quad C_{i1}], i \in \{0, 1, 2\}, B_i = \begin{bmatrix} B_{i0} \\ B_{i1} \end{bmatrix}, i \in \{0, 1\}.$$

the system can be formulated as a differential-algebraic equation of the form

$$A \frac{d}{dt}x(t) + b(x(t), t) = 0.$$

The stand alone equations for the electromagnetic device can be formulated as

$$\begin{aligned} A_0 \begin{pmatrix} \mathcal{V} \\ \mathcal{A} \end{pmatrix} + A_1 \frac{d}{dt} \begin{pmatrix} \mathcal{V} \\ \mathcal{A} \end{pmatrix} + A_2 \frac{d^2}{dt^2} \begin{pmatrix} \mathcal{V} \\ \mathcal{A} \end{pmatrix} + B_0 U + B_1 \frac{d}{dt} U &= 0 \\ C_0 \begin{pmatrix} \mathcal{V} \\ \mathcal{A} \end{pmatrix} + C_1 \frac{d}{dt} \begin{pmatrix} \mathcal{V} \\ \mathcal{A} \end{pmatrix} + C_2 \frac{d^2}{dt^2} \begin{pmatrix} \mathcal{V} \\ \mathcal{A} \end{pmatrix} + D_0 U + D_1 \frac{d}{dt} U + Y &= 0 \end{aligned}$$

whereas  $U = hA_M^T e$  is the applied voltage at the contacts where  $h$  is the auxiliary functions and where  $Y = Lj_M$  is the current through the electromagnetic device. The discretization of Maxwell's equations in space may lead to a system of linear-algebraic equations.

### 3 Nonlinear Coupling

#### 3.1 MNA

The Modified Nodal Analysis leads to a DAE of the following type.

$$A \frac{d}{dt} d(x, t) + b(x, t) = 0$$

where  $A$  is a constant matrix and  $d$  and  $b$  are functions depending on  $x = (e, j_V, j_L)$  and the time  $t$ . For our purposes it suffices to consider  $d(x, t) = d(x)$ .

#### 3.2 EM System

The EM system can be split into two vector valued equations, one corresponding to the Maxwell system (i.e. the discretized Gauss equation and the discretized Maxwell-Ampere equation) and one to the discretized current equation. In the linear case this was the same with the matrices  $A, B, C, D$ . In the nonlinear case we would write these two equations in the following way:

$$\tilde{A} \frac{d}{dt} \tilde{d}(x, t) + \tilde{b}(x, t) = 0 \tag{1}$$

$$\hat{A} \frac{d}{dt} \hat{d}(x, t) + \hat{b}(x, t) = Y \tag{2}$$

Here  $x = (V, \phi_p, \phi_n, A, \Pi, V_{app})$  and  $Y$  is the current through the contacts. Observe here that we moved away from the agreement that we write all equations in the form  $\dots = 0$ . Nevertheless in this case it makes sense to write it like above because then we do not need to use the current  $Y$  as input.

In order to set up a co-simulation approach of a circuit simulator and field solver, the non-linear the field solver will be able to provide the following field data:

- We will use the vector  $x$  being the content of all variables that determines the EM system, e.g.  $x = (V, p, n, A, \Pi, V_{app})$ .
- We will generate a *matrix*  $\mathbf{A} = \tilde{A}$ , e.g. the matrix in front of the operator  $\frac{d}{dt}$  acting on  $x$ .
- We will generate a *vector*  $\mathbf{B}$  that results from evaluating  $\tilde{b}(x)$ .

- We will generate a *matrix*  $\mathbf{C}$  that is needed to evaluate the  $\frac{d}{dt}$  part of  $Y$  in eq. (2). This is  $\hat{A}$ .
- We will generate a *vector*  $\mathbf{D}$  that is needed to evaluate (remaining part of)  $Y$  in eq. (2) This is  $\hat{b}$ .
- We will generate a *matrix*  $\mathbf{J}$  that contains the Jacobian of the  $\tilde{b}$  and  $\hat{b}$  with respect to  $x$ .
- We will generate a *vector*  $\mathbf{X}$  that contains the field state space  $x$  except for the  $V_{app}$ .

In order to get a better insight in the EM equations and how their transient versions are designed, we will present here a detailed derivation. Let us start with the current-continuity equation in metallic regions.

$$\nabla \cdot \mathbf{J} + \frac{\partial \rho}{\partial t} = 0 \quad (3)$$

In here,

$$\rho = \nabla \cdot \mathbf{D} \quad (4)$$

Furthermore,

$$\begin{aligned} \mathbf{E} &= -\nabla V - \frac{\partial \mathbf{A}}{\partial t} \\ \mathbf{\Pi} &= \frac{\partial \mathbf{A}}{\partial t} \\ \mathbf{E} &= -\nabla V - \mathbf{\Pi} \end{aligned} \quad (5)$$

For the nonlinear case MAGWEL has to do the substitution  $\frac{d}{dt}A = \mathbf{\Pi}$ . MECS cannot have the control here. So we need as input here the first order terms represented by  $\tilde{A}$ ,  $\hat{A}$ . The  $\tilde{A}, \hat{A}$  are constant for metal/insulator structures, and so can be put out of the derivative here, For semiconducting domains, we will see that these matrices depend on the local concentrations. Furthermore we need as input the 0th order terms  $\tilde{b}, \hat{b}$ . So we need here

- two matrices  $\tilde{A}, \hat{A}$  and
- two vectors  $\tilde{b}(x), \hat{b}(x)$

which are evaluated at  $x = (V, \phi_p, \phi_n, A, \mathbf{\Pi}, V_{app})$ . The *explicit* time dependency of  $\tilde{d}, \hat{d}, \tilde{b}, \hat{b}$  is not there so we can omit  $t$ . So the final expressions in the most general case are:

$$\tilde{A}(x) \frac{d}{dt} \tilde{d}(x) + \tilde{b}(x) = 0 \quad (6)$$

$$\hat{A}(x) \frac{d}{dt} \hat{d}(x) + \hat{b}(x) = Y \quad (7)$$

For each link the discretized version of  $\mathbf{E}$  is

$$E_{ij} = -\frac{1}{h_{ij}} (V_j - V_i + s_{ij} \mathbf{\Pi}_{ij} h_{ij}) \quad (8)$$

In here,  $s_{ij} = \pm 1$  is depending on the link orientation.

### 3.3 Current-continuity equation discretization in metals

Let  $\sigma_{ij}$  be the conductance associated the the link  $\langle ij \rangle$ . Then the discretized current-continuity equation takes the following form :

$$\sum_j \frac{d_{ij}}{h_{ij}} \varepsilon \frac{\partial}{\partial t} (V_j - V_i + s_{ij} \Pi_{ij} h_{ij}) + \sum_j \frac{d_{ij}}{h_{ij}} \sigma_{ij} (V_j - V_i + s_{ij} \Pi_{ij} h_{ij}) = 0 \quad (9)$$

It is programmed as :

$$\sum_j \frac{d_{ij}}{h_{ij}} \varepsilon \frac{\partial}{\partial t} (V_i - V_j - s_{ij} \Pi_{ij} h_{ij}) + \sum_j \frac{d_{ij}}{h_{ij}} \sigma_{ij} (V_i - V_j - s_{ij} \Pi_{ij} h_{ij}) = 0 \quad (10)$$

In here,  $d_{ij}$  is the dual area corresponding to the link  $\langle ij \rangle$  and  $h_{ij}$  is the length of the link  $\langle ij \rangle$ . From this equation we can read off the content of the matrix  $\tilde{A}$ . Furthermore, the current - continuity equation for metals has the property that the function  $\tilde{d}$  is trivial.

### 3.4 Current-continuity in semiconductors

For the intrinsic semiconductor nodes we must also solve the current-continuity equations

$$\begin{aligned} \frac{\partial}{\partial t} p + \nabla \cdot \mathbf{J}_p + qR &= 0 \\ \frac{\partial}{\partial t} n - \nabla \cdot \mathbf{J}_n + qR &= 0 \end{aligned} \quad (11)$$

For the discretized hole currents we obtain using the Scharfetter-Gummel discretization scheme

$$J_{ij}^p = \mu_p \frac{d_{ij}}{h_{ij}} (p_i B[X_{ij}] - p_j B[-X_{ij}]) \quad (12)$$

where

$$X_{ij} = V_j - V_i + s_{ij} h_{ij} \Pi_{ij} \quad (13)$$

and  $B(x) = x/(e^x - 1)$  is the Bernoulli function. Note that the function  $R = R(p, n)$  is the recombination/generation contribution to the current continuity equation. The MAGWEL solver accounts for Shockley-Read-Hall recombination, Auger recombination/-generation and surface recombination.

The equation for the electron current is :

$$J_{ij}^n = - \mu_n \frac{d_{ij}}{h_{ij}} (n_i B[-X_{ij}] - n_j B[X_{ij}]) \quad (14)$$

The hole equation for node  $i$  is

$$\Delta w_i \frac{\partial}{\partial t} p_i + \sum_j \mu_p \frac{d_{ij}}{h_{ij}} (p_i B[X_{ij}] - p_j B[-X_{ij}]) + R(p_i, n_i) \Delta w_i = 0 \quad (15)$$

In here,  $\Delta w_i$  is the nodal volume. In a slightly modified version it reads with  $n_0$  being the intrinsic concentration :

$$\Delta w_i n_0 \frac{\partial}{\partial t} e^{(\phi_i^p - V_i)} + \sum_j \mu_p \frac{d_{ij}}{h_{ij}} (p_i B[X_{ij}] - p_j B[-X_{ij}]) + R(p_i, n_i) \Delta w_i = 0 \quad (16)$$



Thus the function  $\tilde{d}$  is simply the exponential of the difference of the elementary variables  $\phi^p - V$ .

For the electrons we have :

$$\Delta w_i n_0 \frac{\partial}{\partial t} e^{(V_i - \phi_i^n)} + \sum_j \mu_n \frac{d_{ij}}{h_{ij}} (n_i B[-X_{ij}] - n_j B[X_{ij}]) + R(p_i, n_i) \Delta w_i = 0 \quad (17)$$

The function  $\tilde{d} = e^{(V - \phi^n)}$ .

Besides the subtleties of the discretization that need to be considered at material interfaces, above scheme gives a rather complete overview of the time evolution for the variables  $V, \phi^p, \phi^n$ .

However, so far we have not taken into account optimal scaling of the carrier equations. From solving steady-state problems we learned that it is beneficial to push the continuity equations in numerical range that comes closer to "1" by scaling the equations by the nodal concentrations. For the holes this becomes :

$$\Delta w_i \frac{1}{e^{(\phi_i^p - V_i)}} \frac{\partial}{\partial t} e^{(\phi_i^p - V_i)} + \sum_j \mu_p \frac{d_{ij}}{h_{ij}} \left( B[X_{ij}] - \frac{p_j}{p_i} B[-X_{ij}] \right) + \frac{R(p_i, n_i)}{p_i} \Delta w_i = 0 \quad (18)$$

This brings us to the next 'node in the software-design decision tree'. Should we simplify the first term as :

$$\Delta w_i \frac{1}{e^{(\phi_i^p - V_i)}} \frac{\partial}{\partial t} e^{(\phi_i^p - V_i)} = \Delta w_i \frac{\partial}{\partial t} (\phi_i^p - V_i) \quad (19)$$

or keep it 'as-is' ?

Experience in transient simulations has taught us that the discretization of  $\frac{\partial}{\partial t} (\phi_i^p - V_i)$  induces loss of charge conservation, therefore, we will apply the BDF rules on  $e^{(\phi_i^p - V_i)}$ . If we put everything in the  $n, p$  notation we get here:

$$\Delta w_i \frac{1}{p_i} \frac{\partial}{\partial t} p_i + \sum_j \mu_p \frac{d_{ij}}{h_{ij}} \left( B[X_{ij}] - \frac{p_j}{p_i} B[-X_{ij}] \right) + \frac{R(p_i, n_i)}{p_i} \Delta w_i = 0$$

We see here that the part in front of the time derivative is not constant anymore. This leads to  $\tilde{A}$  not being constant. The fact that we can write

$$\frac{1}{p_i} \frac{\partial}{\partial t} p_i \quad \text{or} \quad \frac{\partial}{\partial t} \ln(p_i)$$

is indeed an important question. Considering the non constant term in front of the time derivative leads to a different formulation of the equations altogether (being a more general one).

For electrons we have

$$\Delta w_i \frac{1}{e^{(V_i - \phi_i^n)}} \frac{\partial}{\partial t} e^{(V_i - \phi_i^n)} + \sum_j \mu_p \frac{d_{ij}}{h_{ij}} \left( B[-X_{ij}] - \frac{n_j}{n_i} B[X_{ij}] \right) + \frac{R(p_i, n_i)}{n_i} \Delta w_i = 0 \quad (20)$$

From the discussion above, it is clear that the communication between the MNA and the EM solver, is effected by the scaling procedure. Fortunately, this is not a show stopper.

At each time instant we can extract from the EM solver the matrices

$$\tilde{A}_{lm} = \Delta w_l E_{lm} e^{-(V_i - \phi_l^n)} \quad (21)$$

where  $E_{lm}$  is the identity (unit) matrix. For holes we get:

$$\tilde{A}_{lm} = \Delta w_l E_{lm} e^{-(\phi_l^p - V_i)} \quad (22)$$

Since the state - space variables  $V, \phi^p, \phi^n$  are known at any instant both in the EM solver and by pointers accessible by the DAEn solver, a conversion to  $p$  and  $n$  can be done 'on-the-fly'. The EM solver will assemble the remainder term  $\tilde{b}$  using the state-space content and the geometrical situation.

### 3.5 Gauss' law

Remember that we could construct the EM system in two ways:

- 1) We exploit the Gauss' law and after a complete discretization, the gauge condition is obtained as a by-product of the solution
- 2) we solve for the gauge condition and the discretized Gauss' law is a by-product of the solution.

Let us purchase the first option. For insulating regions (interior nodes!) we obtain the discretized Gauss' law in the following form

$$\varepsilon \frac{d_{ij}}{h_{ij}} (V_i - V_j - s_{ij} \Pi_{ij} h_{ij}) = 0 \quad (23)$$

Note that there is no term containing a time differentiation. The corresponding content of the  $\tilde{A}$  matrix is zero. Physically, this equation is a *constraint*.

Next let us consider an *interior* semiconductor node. First of all Gauss' law gets modified by a charge contribution.

$$\varepsilon \frac{d_{ij}}{h_{ij}} (V_i - V_j - s_{ij} \Pi_{ij} h_{ij}) - qp_i(\phi_i^p, V_i) \Delta w_i + qn_i(\phi_i^n, V_i) \Delta w_i + qN_D \Delta w_i = 0 \quad (24)$$

in which  $w_i$  is nodal volume and  $N_D$  is the net doping. All time dependence is *implicit*. Therefore, this equation still is a constraint. The hole and electron concentrations are given by

$$\begin{aligned} p &= n_0 \exp(\phi^p - V) \\ n &= n_0 \exp(V - \phi^n) \end{aligned} \quad (25)$$

where  $n_0$  is the intrinsic concentration. The SI unit of  $q$  is [C] = Coulomb and the SI units of  $n$  and  $p$  are  $m^{-3}$ .

### 3.6 Maxwell-Ampere law

Finally, we also consider the Maxwell-Ampere equation. The starting point is

$$\nabla \times \mathbf{H} = \mathbf{J}_c + \mathbf{J}_d \quad (26)$$

Using the  $\mathbf{AV}$  substitutions it becomes :

$$\varepsilon \frac{\partial}{\partial t} \mathbf{\Pi} + \nabla \times \left( \frac{1}{\mu} \nabla \times \mathbf{A} \right) = \mathbf{J}_c - \varepsilon \frac{\partial}{\partial t} (\nabla V) \quad (27)$$

This should be completed with the gauge condition.

$$\frac{1}{\mu_0} \nabla (\nabla \cdot \mathbf{A}) + \xi \varepsilon \nabla \left( \frac{\partial}{\partial t} V \right) = 0 \quad (28)$$

In the discretization procedure, a multiplication with  $\mu_0$  is done as well as a multiplication with the length of the link. This gives

$$\begin{aligned} & \mu_0 L \Delta S_{ij} \varepsilon \frac{\partial}{\partial t} \Pi_{ij} + L \Delta S_{ij} (1 - \xi) \mu_0 \varepsilon \frac{\partial}{\partial t} \nabla V \Big|_{\text{discrete}} \\ & + L \Delta S_{ij} \nabla \times \left( \frac{1}{\mu_r} \nabla \times \mathbf{A} \right) \Big|_{\text{discrete}} - L \Delta S_{ij} \nabla (\nabla \cdot \mathbf{A}) \Big|_{\text{discrete}} \\ & - L \Delta S_{ij} \mu_0 J_{ij}^c = 0 \end{aligned} \quad (29)$$

We can read off straightforwardly the matrix  $\tilde{A}$  from the first two terms as well as the remainder,  $\tilde{b}$ .

So far, we have only considered equation (1). As far as the EM solver is concerned, the second equation is 'post-processing'. However, if the EM module is encapsulated in a larger environment, and moreover, if the environment acts as a 'master' and the EM solver is a 'client' for providing the matrix computation, but no further solving is done, then it is needed that the environment is capable of assigning values to the boundary conditions as well as assigning values to all state-space variables. The role of the EM solver is to provide appropriate values for the matrix and vectors in equation (2). Another way of looking at (2) is

$$Y = \hat{A}(x) \frac{d}{dt} \hat{d}(x) + \hat{b}(x) \quad (30)$$

This looks like a 'stupidity' but the meaning is now clear. Extract the current from the state-space and applied voltages.

### 3.7 Coupled system

Now the coupling takes place by inserting into the MNA equation a relevant term for the EM-Device(s):

$$A \frac{d}{dt} d(x, t) + b(x, t) + \begin{pmatrix} A_M j_M \\ 0 \\ 0 \end{pmatrix} = 0$$

Furthermore we know that the applied potential depends on the node potentials:

$$V_{app} = V_{app}(e)$$

and we have  $Y = Y(j_M)$  being the vector of currents through the contacts.

Our goal later is to write all this together into one (vector-valued) nonlinear equation of the form:

$$f\left(\frac{d}{dt}k(y, t), y, t\right) = 0$$

with  $k(y, t)$  being a nonlinear function and  $y = (e, j_L, j_V, j_M, V, p, n, A, \Pi)$ . This can then be solved with the DAE solvers.

Additionally setting that  $\tilde{d}(x) = \hat{d}(x) = x$  for  $x = (V, p, n, A, \Pi, V_{app}(e))$  we can all put this together into the variables  $(e, j_L, j_V, j_M, V, p, n, A, \Pi)$  as follows:

$$\underbrace{\begin{bmatrix} A & 0 \\ 0 & \tilde{A} \\ 0 & \hat{A} \end{bmatrix}}_{=:A} \frac{d}{dt} \underbrace{\begin{pmatrix} d(e, j_L, j_V, t) \\ (V, p, n, A, \Pi, V_{app}(e))^T \end{pmatrix}}_{=:D(y,t)} + \underbrace{\begin{pmatrix} b(e, j_L, j_V, t) + \begin{pmatrix} A_M j_M \\ 0 \\ 0 \end{pmatrix} \\ \tilde{b}(V, p, n, A, \Pi, V_{app}(e)) \\ \hat{b}(V, p, n, A, \Pi, V_{app}(e)) - Y(j_M) \end{pmatrix}}_{=:B(y,t)} = \begin{pmatrix} 0 \\ 0 \\ 0 \end{pmatrix}$$

So defining  $k(y, t) := D(y, t)$  and with  $\frac{d}{dt}k(y, t) = w$  we write

$$f(w, y, t) := Aw + B(y, t)$$

### 3.8 Technical realization

Fig. 3 gives a good overview of the whole coupling idea between the MECS solver and the EM solver.

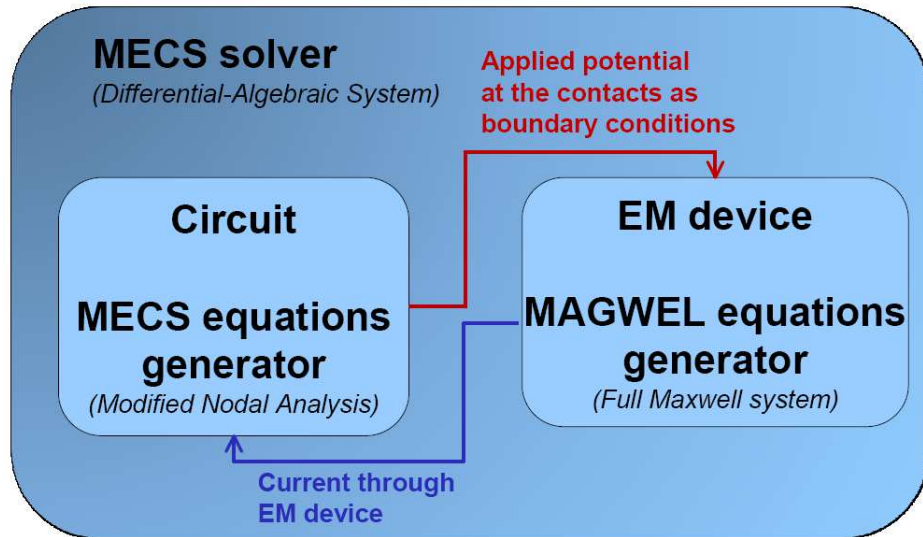


Figure 3: Coupling MECS solver with EM.

On the technical level one has to specify how the two software packages interact (Fig. 4). Since the MECS solver is written in Python and the EM solver in C/C++ we use Cython as a communication bridge, cf. <http://cython.org/>. Cython is a programming language which understands both C/C++ code and Python code and it is possible to exchange data types. The data exchange is realized via pointers to vectors and matrices. The EM solver functionality is available via a shared library.

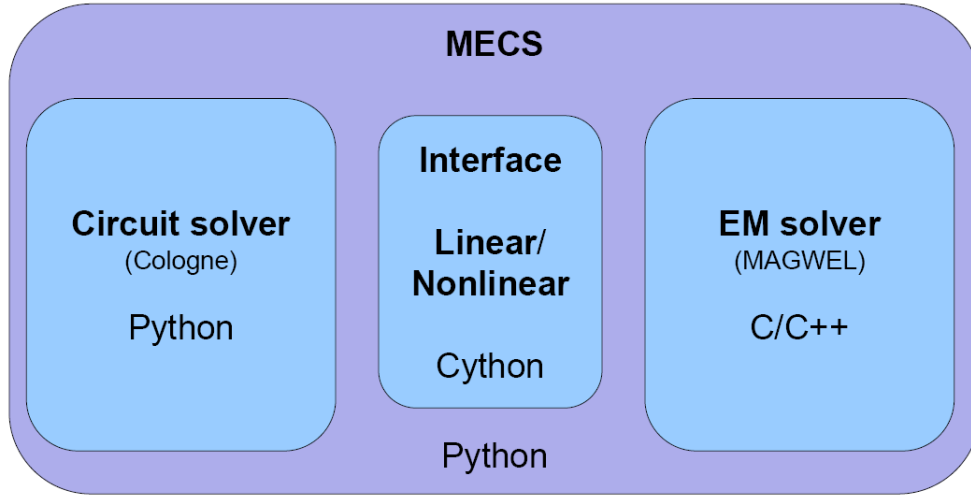


Figure 4: Technical coupling MECS solver with EM via Cython.

In the following we will highlight the calling order of the nonlinear interface a little bit more.

- The first step is that MECS starts the EM solver via the function

```
char** magwel_nonlinear_init(char *model){
    constructSolvEMAPI( model );

    int nrLinks = getNrLinks();
    int nrNodes = getNrNodes();
    int nrSemiconductorNodes = getNrSemiconductorNodes();
    int nrContacts = getNrContacts();
    int sizeV = getSizeV();
    int sizeP = getSizeP();
    int sizeN = getSizeN();
    int sizeA = getSizeA();
    int sizePi = getSizePi();
    int sizeVappl = getSizeVappl();

    ...

    return init_array_pointers;
}
```

It constructs the API for the EM solver and as init information returns the number of nodes, links, etc. This information is needed to construct the matrices in the MECS solver with the right dimensions.

- Running through the time integrator an update for a new input at a new time point is needed. So the matrices  $\tilde{A}$ ,  $\hat{A}$ ,  $\tilde{b}$ ,  $\hat{b}$  need to be extracted from the EM part. It

is also convenient for the MECS solver to have the Jacobian available to solve the implicit BDF scheme. All this is done with the function

```

char** magwel_nonlinear_update(char *model, double *input_V ,
                               double *input_p ,double *input_n ,
                               double *input_A ,double *input_Pi ,
                               double *input_Vapp){
    ...

    loadStateVariables( input_array_pointers );

    computeStateSpace ();

    constantPartEM_matrix = getConstantPartEM ();

    staticPartMaxwellEM_array = getDiscretizedStaticMaxwellEM ();
    staticPartCurrentEM_array = getDiscretizedStaticCurrentEM ();

    Jacobian_array = getDiscretizedJacobian ();

    stateSpace_array = getStateSpaceSolution ();

    confirmResultsRead ();
    ...

    return output_array_pointers ;
}

```

First the state variables ( $x$ ) are loaded into the EM solver and then the full Maxwell system is solved (`computeStateSpace()`). The output is then extracted in the form of  $\tilde{A}$ ,  $\hat{A}$ ,  $\tilde{b}$ ,  $\hat{b}$  and  $J$

- The nonlinear interface also provides a stopping function which shuts down the EM solver because it is not needed anymore. It takes care of memory deallocation in the EM solver part.

```

void magwel_nonlinear_stop () {

    deallocateStateMatrices ();

    destroySolvEMAPI ();

    return ;
}

```

The linear interface works about the same. The main difference here is that we exchange only matrices and that we need to call the update function only once.

## 4 Constructing the output vector $Y$

The observables  $Y$  are part of the complete model. In the present model we take the currents at the contacts as the observables of the state space. Furthermore, the currents are defined as positive ( $> 0$ ), when the current is outgoing of the simulation domain. In particular,  $Y = \{I_1, I_2, \dots, I_{nc}\}$ . We will now present the detailed derivation of the matrices  $Y$ . Our starting point will be the current-continuity equations for the contact nodes. The

current continuity can be expressed as :

$$\nabla \cdot \mathbf{J} = 0 \quad \text{where} \quad \mathbf{J} = \mathbf{J}_{\text{cond}} + \mathbf{J}_{\text{disp}} \quad (31)$$

For a contact node the discrete assembling gives

$$\sum_j d_{ij} J_{ij} + I_i^{\text{out}} = 0 \quad (32)$$

In Fig. 5 this is illustrated.

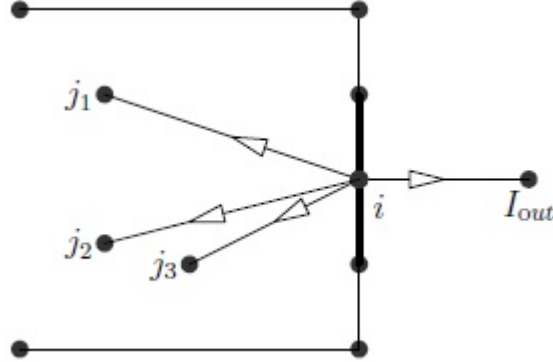


Figure 5: Illustration of the currents at a contact node,  $i$ . The nodes  $j$  are field nodes.

The total current for the contact is obtained by summing over all the contact nodes :

$$I^{\text{out}} = \sum_i I_i^{\text{out}} \quad (33)$$

The assembling of the current-continuity equations for internal nodes,  $j$ , runs over all links that are connected to  $j$ , including the contact nodes  $i$ . Whereas in the stand-alone field solving approach these contributions are not considered for the matrix building, we can evaluate these contributions for the construction of the matrices  $C$  and  $D$ . Using the fact that  $J_{ij} = -J_{ji}$ , the assembling leads to the following result :

$$\begin{aligned} & - \sum_j \frac{d_{ij}}{h_{ij}} \sigma V_j + \sum_j \frac{d_{ij}}{h_{ij}} \sigma V_i - \sum_j d_{ij} \sigma s_{ij} \frac{\partial}{\partial t} A_{ij} \\ & - \sum_j \frac{d_{ij}}{h_{ij}} \frac{\partial}{\partial t} (\epsilon V_j) + \sum_j \frac{d_{ij}}{h_{ij}} \frac{\partial}{\partial t} (\epsilon V_i) \\ & - \sum_j d_{ij} s_{ij} \frac{\partial^2}{\partial t^2} (\epsilon A_{ij}) + I_i^{\text{out}} = 0 \end{aligned} \quad (34)$$

We have observed that the use of second order time differentiation can be completely

avoided by using the variable  $\mathbf{\Pi}$  in equation (34). Then this equation becomes

$$\begin{aligned}
& - \sum_j \frac{d_{ij}}{h_{ij}} \sigma V_j + \sum_j \frac{d_{ij}}{h_{ij}} \sigma V_i - \sum_j d_{ij} \sigma s_{ij} \Pi_{ij} \\
& \quad - \sum_j \frac{d_{ij}}{h_{ij}} \frac{\partial}{\partial t} (\epsilon V_j) + \sum_j \frac{d_{ij}}{h_{ij}} \frac{\partial}{\partial t} (\epsilon V_i) \\
& \quad - \sum_j d_{ij} s_{ij} \frac{\partial}{\partial t} (\epsilon \Pi_{ij}) + I_i^{\text{out}} = 0
\end{aligned} \tag{35}$$

Therefore, for a contact for which the nodes are in the collection  $i_C$  we obtain

$$\begin{aligned}
I_{i_C}^{\text{out}} &= \sum_{i \in i_C, j} \frac{d_{ij}}{h_{ij}} \sigma (V_j - V_i) + \sum_{i \in i_C, j} d_{ij} \sigma s_{ij} \Pi_{ij} \\
& \quad + \sum_{i \in i_C, j} \frac{d_{ij}}{h_{ij}} \frac{\partial}{\partial t} (\epsilon (V_j - V_i)) + \sum_{i \in i_C, j} d_{ij} s_{ij} \frac{\partial}{\partial t} (\epsilon \Pi_{ij})
\end{aligned} \tag{36}$$

It is interesting to note that for a contact attached to an insulating region we can also use equation (36) and set  $\sigma = 0$ . It becomes then

$$I_{i_C}^{\text{out}} = \sum_{i \in i_C, j} \frac{d_{ij}}{h_{ij}} \frac{\partial}{\partial t} (\epsilon (V_j - V_i)) + \sum_{i \in i_C, j} d_{ij} s_{ij} \frac{\partial}{\partial t} (\epsilon \Pi_{ij}) \tag{37}$$

For contacts attached to semiconducting domains we must use the sum of the hole and electron currents. Starting from

$$\nabla \cdot (\mathbf{J}^p + \mathbf{J}^n) + \frac{\partial}{\partial t} (p - n) = 0 \tag{38}$$

we get

$$\begin{aligned}
I_{i_C}^{\text{out}} &= - \sum_{i \in i_C, j} d_{ij} (J_{ij}^p + J_{ij}^n) \\
& \quad + \sum_{i \in i_C, j} \frac{d_{ij}}{h_{ij}} \frac{\partial}{\partial t} (\epsilon (V_j - V_i)) + \sum_{i \in i_C, j} d_{ij} s_{ij} \frac{\partial}{\partial t} (\epsilon \Pi_{ij})
\end{aligned} \tag{39}$$

## 5 Testing the non-linear interface

### 5.1 Testing the Jacobian $J$

In order to check the result of the non-linear interface, we use an elementary test case consisting of a metal pillar contained in oxide. The structure and the mesh are shown in Fig. 6.

The structure has three contacts. The side contacts are electrically identical. That means they are all represented by one row in the equation assembling. The side contacts are inserted in order to lower the number of node degrees of freedom.

It should be stressed that we have now a field device with more than two contacts. In general the field device can have  $N$  contacts and only a subset  $k < N$  are included in the



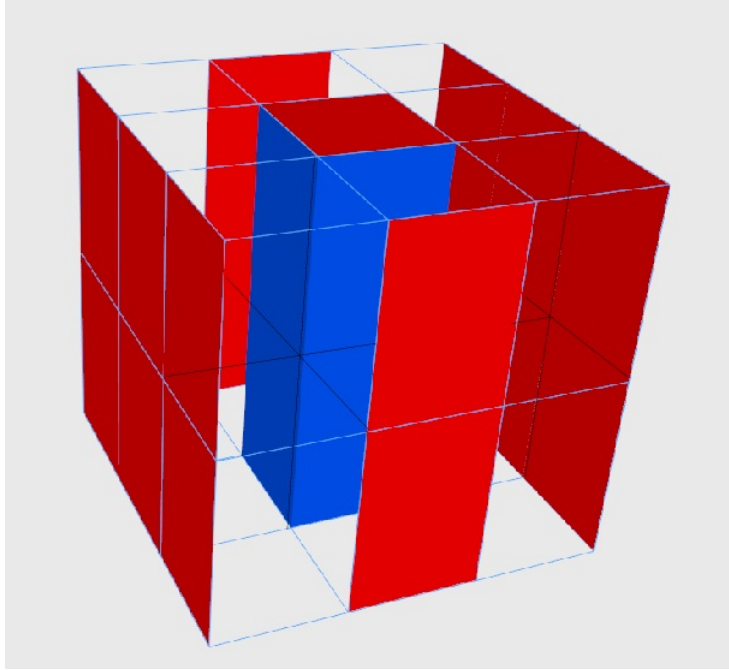


Figure 6: Test structure design: a simple pillar with mesh. The out surface is covered with contacts to reduce the DOF count.

coupling. By this we mean that a corresponding node is allocated in the MECS solver. The contacts  $k, k + 1, \dots, N$  are assumed to be grounded. The grounded contacts do not participate in the set up of the coupled equation system. If a corresponding node is identified in the MECS solver, then the treatment of the contact is always done following the current-continuity. In general we can imagine several use models:

- *all* contacts are addressed in MECs via some connecting element,
- a *subclass* of contacts is addressed in MECS. Others are addressed and fixed in DEVEM,
- Contacts in devEM may not be directly attached to voltage or current sources of the MNA net list.

A complexity arises if the equation set up in devEM depends on the fact if an applied voltage (voltage source) is attached to a contact that is itself glued to an insulating region. In this situation, the applied voltage is eliminated from the vector  $\mathbf{x}$ . We can avoid this complexity by always inserting a metal region and attach the contact to the metal region, In this test case this is not done since here we want to keep the number of degrees of freedom as small as possible.

*For the time being, we will use the non-linear interface exclusively in such a way that all device contacts of the field solving part will be driven by nodes of the MECS solver.*

The nodal degrees of freedom are located in the horizontal cut plane in the middle. Furthermore, only links in the z-direction are contributing to the collection of degrees of freedom, There are 8 links located at the vertical edges of the metal pillar where there are degrees of freedom. The total set of variables is 23 being :

$\{V_1, V_2, V_3, V_4, A_1, A_2, A_3, A_4, A_5, A_6, A_7, A_8, \Pi_1, \Pi_2, \Pi_3, \Pi_4, \Pi_5, \Pi_6, \Pi_7, \Pi_8, V_{C1}, V_{C2}, V_{C3}\}$   
 There are 20 degrees of freedom and 3 contact variables. In Fig. 7 we see the time-dependent solutions via the nonlinear interface for the benchmark structure given in 6 when a voltage source of a pulse source starting from zero to 3V is applied to the top and down contact areas of the metal (blue) part. In Fig. 8 we see the results for a sinoidal source. Due to the initial zero status for the field solver, the applied voltages source is chosen such that it starts linearly from zero before behaving sinoidal between 3V and 9V.

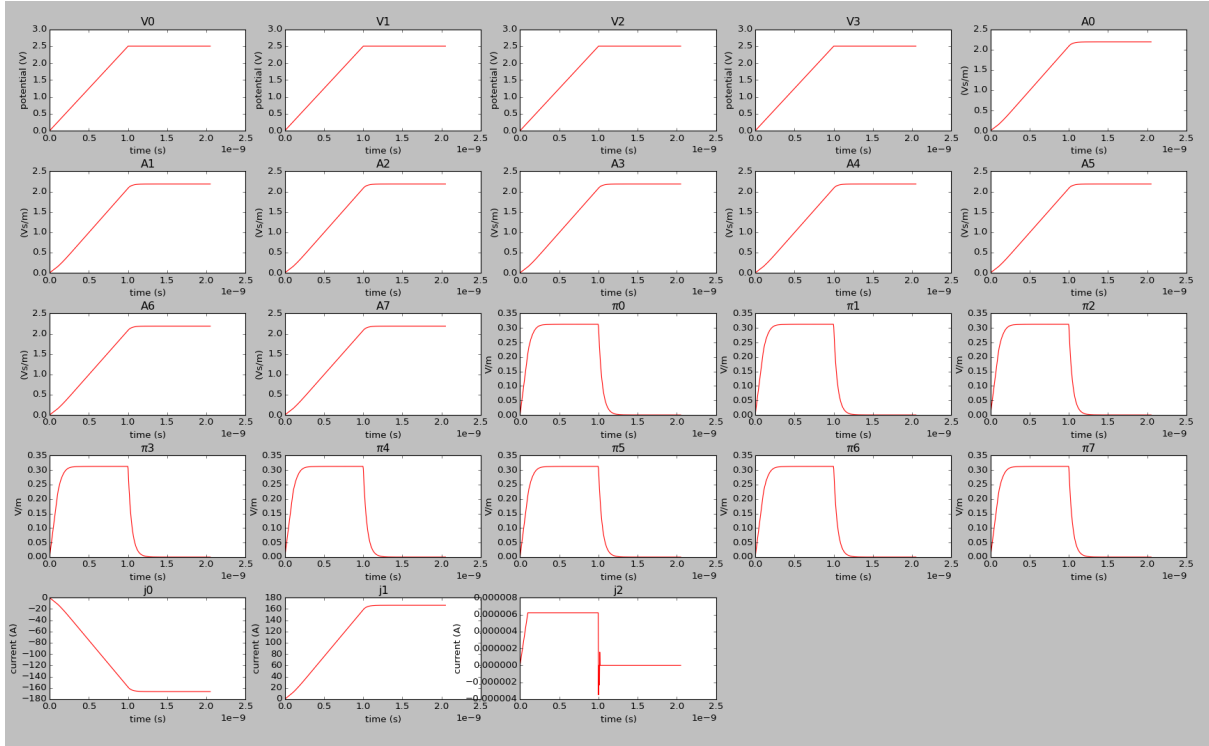


Figure 7: Computed solutions for the test benchmark given in Fig. 6 with a pulse voltage source applied. The first four images (reading line by line) show the scalar potentials  $V_i$ . The next 8 images show the vector potentials  $A_i$  along the 8 inner grid lines belonging to the silicon oxid. Thereafter, one sees the time derivatives  $\pi_i = \partial_t A_i$  of the 8 vector potentials. Finally, the last three images show the currents  $j_0$  and  $j_1$  through the top and down contact areas as well as the almost vanishing substrat current  $j_2$  through the other (red) contact areas connected to ground.

Note that the Jacobians are filled up to a maximum row and column index of 23 (see Fig. 9 and Fig. 10). This is due to the fact that the 3rd contact is glued on an insulating domain. As a consequence the assembling of the 3rd contact contributes to  $\hat{a}$ . Before interpreting the values we must first discuss the scaling schemes that are exploited. For the time being it suffices to say that the matrix elements are all in SI units.

The scaled Jacobians for one arbitrarily chosen time point are given in Fig. 9 for the pulse source and in Fig. 10 for the sinoidal source. They are sparse but demanding because of their high condition number. Row scalings lead to a condition number of order  $10^{10}$  and  $10^7$ , respectively.

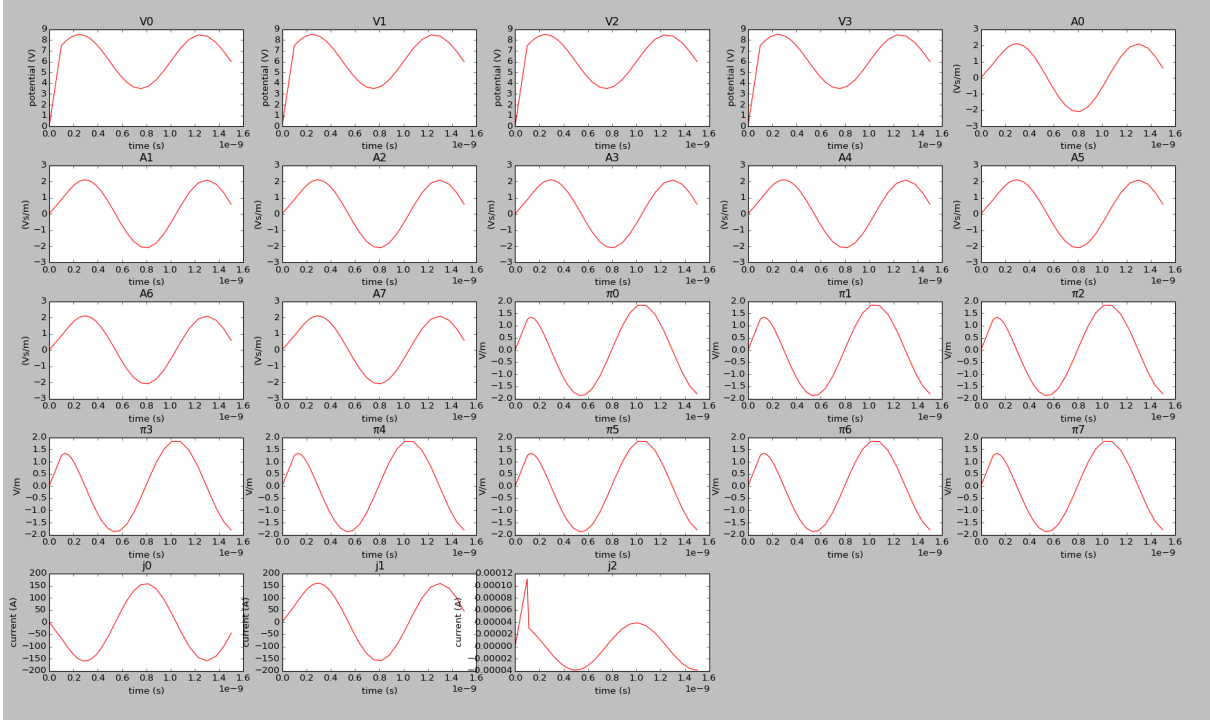


Figure 8: Computed solutions for the test benchmark given in Fig. 6 with a sinoidal voltage source applied. At the beginning the voltage source starts linearly from zero before being sinusoidal between 3V and 6V. The first four images (reading line by line) show the scalar potentials  $V_i$ . The next 8 images show the vector potentials  $A_i$  along the 8 inner grid lines belonging to the silicon oxid. Thereafter, one sees the time derivatives  $\pi_i = \partial_t A_i$  of the 8 vector potentials. Finally, the last three images show the currents  $j_0$  and  $j_1$  through the top and down contact areas as well as the almost vanishing substrat current  $j_2$  through the other (red) contact areas connected to ground.

## 5.2 Scaling choices

Scaling is a major issue in the technical debugging process. In order to clarify the situation here we present a short overview of scaling choices for a Differential-Algebraic Equation. We distinguish between three types of scaling:

- Scaling of variables
- Scaling of time
- Scaling of equations

We start with the completely unscaled equation

$$A(x_u(t_u)) \frac{d}{dt_u} x_u(t_u) + b(x_u(t_u)) = 0$$

for the unscaled input  $x_u$  at the unscaled time  $t_u$ . Now introducing the variable scaling

$$Sx_s = x_u$$

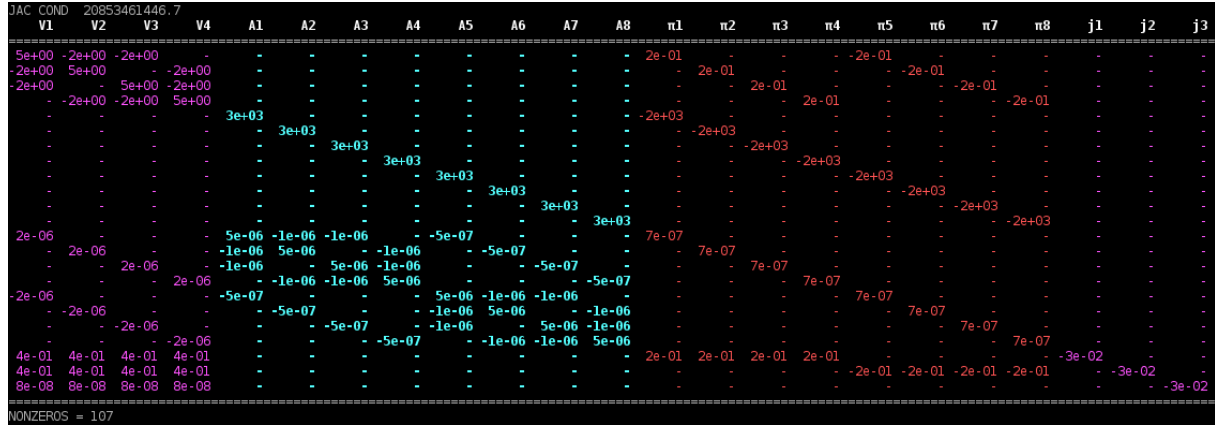


Figure 9: Jacobian for the test benchmark given in Fig. 6 with a pulse voltage source applied. After row scaling we have the condition number of  $2.09 \cdot 10^{10}$ .

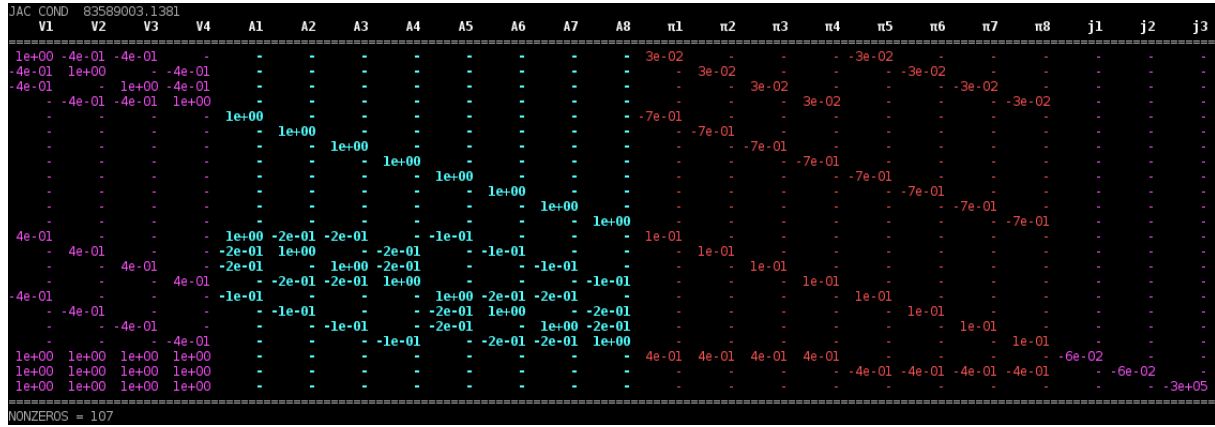


Figure 10: Jacobian for the test benchmark given in Fig. 6 with a sinoidal voltage source applied. After row scaling we have a condition number of  $8.36 \cdot 10^7$ .

where  $S$  is a diagonal matrix which is fixed for all times we get equivalently

$$A(Sx_s(t_u)) \frac{d}{dt_u} (Sx_s(t_u)) + b(Sx_s(t_u)) = 0.$$

Now we put the time scaling into play via

$$t_s = \alpha t_u$$

with the scaling factor  $\alpha$ . Defining

$$\tilde{x}_s(t_s) := x_s(\alpha t_s)$$

and using that

$$\frac{d}{dt_u} (x_s(t_u)) = \frac{d\tilde{x}_s}{dt_s} \frac{dt_s}{dt_u} = \alpha \frac{d\tilde{x}_s}{dt_s}$$

we get

$$\alpha A(S\tilde{x}_s(t_s)) S \frac{d}{dt_s} (\tilde{x}_s(t_s)) + b(S\tilde{x}_s(t_s)) = 0.$$

which is then the scaled equation. Notice that we did not use scaling of equations here which is basically multiplying every row by a specific factor which is independent of time and the variables. We assume here that this is already done when producing  $A$  and  $b$ .

Another way of addressing scaling is to start from the equations that are solved. These are

- The current-continuity equations
- Gauss' law
- The Maxwell-Ampere equation

There are two ways to arrive at the solution: the first method starts from the continuous field equations and performs the scaling at this level as illustrated above and next starts the discretization process acting on the scaled equations. There is also the other approach, where we first discretize the equations and next perform the scaling. Of course both approaches are equally valid but in order to study coupled systems, the second approach is more transparent. It is the second approach that we will pursue here.

For the current-continuity equation we start from the formulation as it is programmed (see equation (40))

$$\sum_j \frac{d_{ij}}{h_{ij}} \varepsilon \frac{\partial}{\partial t} (V_i - V_j - s_{ij} \Pi_{ij} h_{ij}) + \sum_j \frac{d_{ij}}{h_{ij}} \sigma_{ij} (V_i - V_j - s_{ij} \Pi_{ij} h_{ij}) = 0 \quad (40)$$

The SI unit of each term is  $[A] = \text{Ampere}$ .

For Gauss' law we start from :

$$\varepsilon \frac{d_{ij}}{h_{ij}} (V_i - V_j - s_{ij} \Pi_{ij} h_{ij}) - qp_i(\phi_i^p, V_i) \Delta w_i + qn_i(\phi_i^n, V_i) \Delta w_i + qN_D \Delta w_i = 0 \quad (41)$$

In insulators it reads :

$$\varepsilon \frac{d_{ij}}{h_{ij}} (V_i - V_j - s_{ij} \Pi_{ij} h_{ij}) = 0 \quad (42)$$

The SI unit of each term is  $(C^2)/(Nm^2) \cdot V/m \cdot m^2$ . Since  $V = Nm/C$ , the SI unit of each term is  $[C] = \text{Coulomb}$ .

In semiconductors we have

$$\varepsilon \frac{d_{ij}}{h_{ij}} (V_i - V_j - s_{ij} \Pi_{ij} h_{ij}) - qp_i(\phi_i^p, V_i) \Delta w_i + qn_i(\phi_i^n, V_i) \Delta w_i + qN_D \Delta w_i = 0 \quad (43)$$

where  $n_0$  is the intrinsic concentration. The SI unit of  $q$  is  $[C] = \text{Coulomb}$  and the SI units of  $n$  and  $p$  is  $m^{-3}$ . Therefore each term has dimension  $[C]$ .

For the Maxwell-Ampere equation the starting formulation is (see equation (29)) :

$$\begin{aligned}
& \mu_0 L \Delta S_{ij} \varepsilon \frac{\partial}{\partial t} \Pi_{ij} + L \Delta S_{ij} (1 - \xi) \mu_0 \varepsilon \frac{\partial}{\partial t} \nabla V \Big|_{\text{discrete}} \\
& + L \Delta S_{ij} \nabla \times \left( \frac{1}{\mu_r} \nabla \times \mathbf{A} \right) \Big|_{\text{discrete}} - L \Delta S_{ij} \nabla (\nabla \cdot \mathbf{A}) \Big|_{\text{discrete}} \\
& - L \Delta S_{ij} \mu_0 J_{ij}^c = 0 \quad (44)
\end{aligned}$$

The term  $L \Delta S_{ij} (1 - \xi) \mu_0 \varepsilon \frac{\partial}{\partial t} \nabla V \Big|_{\text{discrete}}$  allows us to evaluate the dimension of each term as  $m \cdot m^2 \mu_0 \varepsilon_0 \cdot V / (m \text{sec})$ . The dimension of  $\mu_0 \varepsilon_0$  is equal to dimension of  $1/c^2$  which is  $\text{sec}^2/m^2$  ( $c = \text{speed of light}$ ). Therefore the dimension of each term in the discretized Maxwell-Ampere equation is  $V \text{sec}$ . We can easily confirm this from the 4th and 5th term. These terms have dimension  $m m^2 m^{-1} m^{-1} \text{dim}(\mathbf{A}) = m (V \text{sec}/m) = [V \text{sec}]$ .

Now remember that in the discretization procedure we multiplied to starting Maxwell-Ampere equation with  $\mu_0 = 4\pi \times 10^{-7} \text{mkg}/\text{C}^2$ . Therefore, we may annihilate this multiplication when interfacing the Maxwell-Ampere equation to the non-linear interface. In other words: the *unscaled* equation that is used when describing the Maxwell-Ampere equation will take the following form ;

$$\begin{aligned}
& L \Delta S_{ij} \varepsilon \frac{\partial}{\partial t} \Pi_{ij} + L \Delta S_{ij} (1 - \xi) \varepsilon \frac{\partial}{\partial t} \nabla V \Big|_{\text{discrete}} \\
& + L \Delta S_{ij} \nabla \times \left( \frac{1}{\mu} \nabla \times \mathbf{A} \right) \Big|_{\text{discrete}} - \frac{1}{\mu_0} L \Delta S_{ij} \nabla (\nabla \cdot \mathbf{A}) \Big|_{\text{discrete}} \\
& - L \Delta S_{ij} J_{ij}^c = 0 \quad (45)
\end{aligned}$$

### 5.3 Number inspection of the Jacobian

We are now ready to verify the matrix entries. The first 4 rows correspond to current-continuity equations in the metal nodes.

```

%%MatrixMarket matrix coordinate real general
% number of non-zeros: 110
%
%      row      col      value
23      22      110
1        1      183.15
1        2      -74.9249999999999
1        3      -74.925
1       13      7.49249999999999e-05
1       17      -7.49249999999999e-05
1       21      -16.65
1       22      -16.65
2        1      -74.9249999999999
2        2      183.15
2        4      -74.925
2       14      7.49249999999999e-05
2       18      -7.49249999999999e-05
2       21      -16.65
2       22      -16.65
3        1      -74.925
3        3      183.15
3        4      -74.925
3       15      7.4925e-05
3       19      -7.4925e-05

```

3	21	-16.65
3	22	-16.65
4	2	-74.925
4	3	-74.925
4	4	183.15
4	16	7.4925e-05
4	20	-7.4925e-05
4	21	-16.65
4	22	-16.65

The entries (1,2) is a coupling generated by a voltage difference between node 1 and node 2 (new numbering scheme) . The value is  $O(\text{micron}^2)/O(\text{micron}) \cdot O(\text{metalconductance}) = 10^{-12} \cdot 10^6 \cdot 10^8 = O(10^2)$ . The precise results is based in the fact that the matrix element is

$$\frac{\partial \tilde{b}_1}{\partial V_2} = -\frac{d_{12}}{h_{12}} \sigma = -2 \cdot (4.5/2) \cdot 10^{-6} \cdot 1.5 \cdot 10^{-6} / (3.0 \cdot 10^{-6}) \cdot 0.333 \cdot 10^8 = -74.925 \quad (46)$$

The dimension of this matrix element is  $A/V = \Omega^{-1} = S$ . Next we consider the matrix element (1,13). The equation is with  $x_{13} = \Pi_1$ ,

$$\frac{\partial \tilde{b}_1}{\partial \Pi_1} = -d_{12} s_{12} \sigma = 1.5 \cdot 10^{-6} \cdot 1.5 \cdot 10^{-6} \cdot 0.333 \cdot 10^8 = -s_{12} 0.74925 \cdot 10^{-4} = -s_{12} \cdot 7.4925 \cdot 10^{-5} \quad (47)$$

The dimension of this matrix element is  $Sm$ . The sign of the matrix element is determined by the orientation of the link in the grid,  $s_{ij}$ . The link is pointing upwards from the bottom contact to the node and we view the link from the node. Therefore  $s_{ij} = -1$ . Finally, we consider the connection to the bottom contact. It is represented by the matrix element (1, 21) . The equation is

$$\frac{\partial \tilde{b}_1}{\partial x_{21}} = \frac{\partial \tilde{b}_1}{\partial V_{C1}} = -\frac{d_{1,C1}}{h_{1,C1}} \sigma = -1.5 \cdot 10^{-6} \cdot 1.5 \cdot 10^{-6} / (4.5 \cdot 10^{-6}) \cdot 0.333 \cdot 10^8 = -16.65 \quad (48)$$

and its dimension is also  $S$ . Finally, we consider the coupling to the contact C3 at the side wall. This is the matrix element (1,23). The coupling takes place via an insulator cube. We are assembling a current-continuity equation of the type equation (10), with  $\sigma = 0$ . As a result this contribution to the assembling is zero and we expect that  $\frac{\partial \tilde{b}_1}{\partial x_{23}} = 0$ . Finally, the matrix element (1,1) = -(1,2)-(1,3)-(1,21)-(1,22) .

Next we proceed with the rows (5-12). They correspond to the equation for the vector potential  $\mathbf{A}$ .

5	13	-1
6	14	-1
7	15	-1
8	16	-1
9	17	-1
10	18	-1
11	19	-1
12	20	-1

The equation is

$$\frac{\partial A_{ij}}{\partial t} - \Pi_{ij} = 0 \quad (49)$$

Therefore for the element (5,13) we obtain

$$\frac{\partial \tilde{b}_5}{\partial x_{13}} = \frac{\partial \tilde{b}_5}{\partial \Pi_1} = -1 \quad (50)$$

The dimension of the equation is [V/m] matrix element is 1 (dimensionless).

We finally consider the Maxwell-Ampere equations. They are in contained in row 13-20.

13	1	7.492499999999999e-05
13	5	15.9154943091895
13	6	-3.58098621956764
13	7	-3.58098621956764
13	9	-1.59154943091895
13	13	3.371624999999999e-10
13	21	-7.492499999999999e-05
14	2	7.492499999999999e-05
14	5	-3.58098621956764
14	6	15.9154943091895
14	8	-3.58098621956764
14	10	-1.59154943091895
14	14	3.371624999999999e-10
14	21	-7.492499999999999e-05
15	3	7.4925e-05
15	5	-3.58098621956764
15	7	15.9154943091895
15	8	-3.58098621956764
15	11	-1.59154943091895
15	15	3.371625e-10
15	21	-7.4925e-05
16	4	7.4925e-05
16	6	-3.58098621956764
16	7	-3.58098621956764
16	8	15.9154943091895
16	12	-1.59154943091895
16	16	3.371625e-10
16	21	-7.4925e-05
17	1	-7.492499999999999e-05
17	5	-1.59154943091895
17	9	15.9154943091895
17	10	-3.58098621956764
17	11	-3.58098621956764
17	17	3.371624999999999e-10
17	22	7.492499999999999e-05
18	2	-7.492499999999999e-05
18	6	-1.59154943091895
18	9	-3.58098621956764
18	10	15.9154943091895
18	12	-3.58098621956764
18	18	3.371624999999999e-10
18	22	7.492499999999999e-05
19	3	-7.4925e-05
19	7	-1.59154943091895
19	9	-3.58098621956764
19	11	15.9154943091895
19	12	-3.58098621956764
19	19	3.371625e-10
19	22	7.4925e-05
20	4	-7.4925e-05
20	8	-1.59154943091895



20	10	-3.58098621956764
20	11	-3.58098621956764
20	12	15.9154943091895
20	20	3.371625e-10
20	22	7.4925e-05

We will now consider the element (13,1). It corresponds to the coupling of  $\Pi - V$ . Referring to eq(45)

$$\begin{aligned}
& L \Delta S_{ij} \varepsilon \frac{\partial}{\partial t} \Pi_{ij} + L \Delta S_{ij} (1 - \xi) \varepsilon \frac{\partial}{\partial t} \nabla V \Big|_{\text{discrete}} \\
& + L \Delta S_{ij} \nabla \times \left( \frac{1}{\mu} \nabla \times \mathbf{A} \right) \Big|_{\text{discrete}} - \frac{1}{\mu_0} L \Delta S_{ij} \nabla (\nabla \cdot \mathbf{A}) \Big|_{\text{discrete}} \\
& - L \Delta S_{ij} J_{ij}^c = 0 \quad (51)
\end{aligned}$$

and taking  $J_{ij}^c = \sigma_{ij} \left( \frac{V_i - V_j}{h_{ij}} - \Pi_{ij} \right)$ , as well as working in the Lorenz gauge ( $\xi = 1$ ), we obtain

$$\frac{\partial \tilde{b}_{13}}{\partial x_1} = \frac{\partial \tilde{\Pi}_1}{\partial V_1} = -L \Delta S_1 \sigma \frac{1}{h_1} = -\Delta S_1 \sigma \quad (52)$$

Filing the numbers now:  $\Delta S_1 = 1.5 \times 1.5 \mu m^2$  and  $h_1 = L = 4.5 \mu m$ . Furthermore,  $\sigma = 0.333 \times 10^8 S/m$  we find for the element (1,1):  $-1.5 \times 1.5 \times 0.333 \times 10^{-12} m^2 \times 10^8 S/m = -0.74925 \times 10^{-4} Sm$ .

The element (13,13) is originating from the conduction term:

$$\frac{\partial \tilde{b}_{13}}{\partial x_{13}} = \frac{\partial \tilde{\Pi}_1}{\partial \Pi_1} = L \Delta S_1 \sigma \quad (53)$$

Filing the numbers now:  $\Delta S_1 = 1.5 \times 1.5 \mu m^2$  and  $h_1 = L = 4.5 \mu m$ . we find  $4.5 \times 1.5 \times 1.5 \times 0.333 \times 10^{-18} m^3 \times 10^8 S/m = 3.371625 \times 10^{-10} Sm^2$

The elements (14,2), (15,3), (16,4) are analogously explained. The elements (17,1), (18,2), (19,3) and (20,4) are explained in the same way except for a sign change because the link is oriented in a different way with respect to the node. The elements (13,21), (14,21), (15,21), (16,21), (17,22), (18,22), (19,22) and (20,22) can also be understood in this way. (These are couplings to contact voltages).

Next we must check the elements (13,5), (13,6), (13,7), (13,8). These are couplings the vector potentials on the links. First we note that (13,5) = -2 { (13,6) + (13,7) } - (13,8). This can be understood from the fact that on a Cartesian grid the combined operator

$$\nabla \times (\nabla \times \mathbf{A}) \Big|_{\text{discrete}} - \nabla (\nabla \cdot \mathbf{A}) \Big|_{\text{discrete}} = -\nabla^2 \mathbf{A} \Big|_{\text{discrete}} \quad (54)$$

and may be viewed then as a Laplacian. In each direction we have then

$$\frac{d^2 A_i}{dx_j^2} = \frac{2}{h_{j+} + h_{j-}} \left[ \frac{A_i(x + \mathbf{e}_j) - A_i(x)}{h_{j+}} - \frac{A_i(x) - A_i(x - \mathbf{e}_j)}{h_{j-}} \right] \quad (55)$$

In the vertical direction there is only a coupling upwards such that factor -2 is not acting on (13,8) in above expression. The elements (13,6) and (13,7) are evaluated with  $h_{j+} = h_{j-} = 3\mu m$  leading to

$$-\frac{2}{3+3} \times \left(\frac{1}{3} + \frac{1}{3}\right) \times 4.5 \times 1.5^2 \times \frac{1}{4\pi \times 10^{-7}} \mu\text{mC}^2/\text{mkg} = -0.179049 \times 10 \text{ C}^2/\text{kg} \quad (56)$$

This number needs to be multiplied with 2 because two cubes contribute. So  $\Delta S_{ij} = 2 \times 1.5^2 \mu\text{m}^2$ . Therefore the final outcome is  $-3.580989244 \text{ C}^2/\text{kg}$ . The unit can be converted to  $\text{C}^2/\text{kg} = \text{Sm}^2/\text{sec}$ , This completes out number checking.

#### 5.4 Number inspection of $\tilde{A}$ , $\hat{A}$ , $\tilde{b}$ and $\hat{b}$

The number inspection of the other parts of the non-linear interface is done in the same way as above. For example the inspection of  $\tilde{b}$  and  $\hat{b}$  is illustrated in Fig. 11 and Fig. 12. The values are the same as used in the prior section.

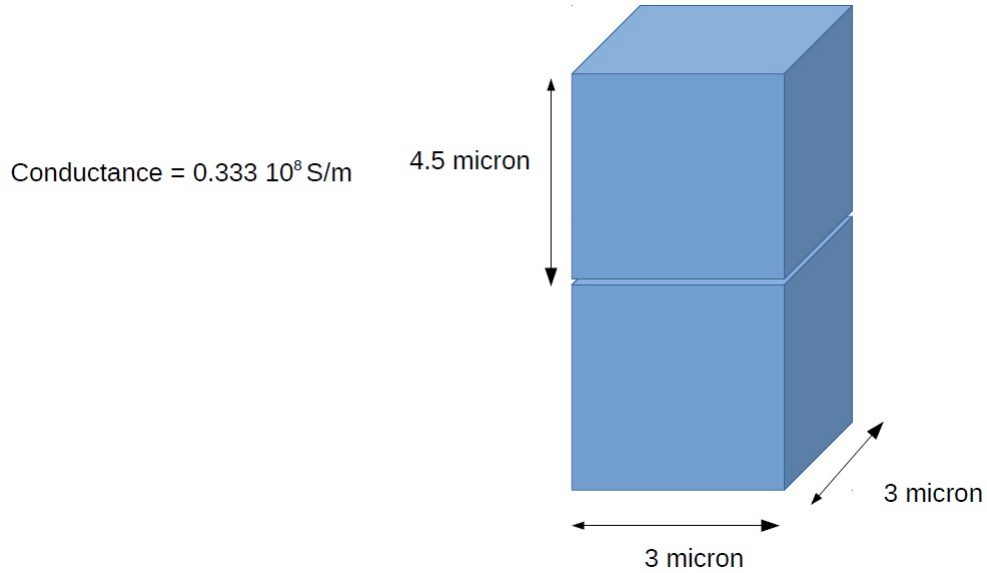


Figure 11: illustration of one mesh volume and its dimensions.

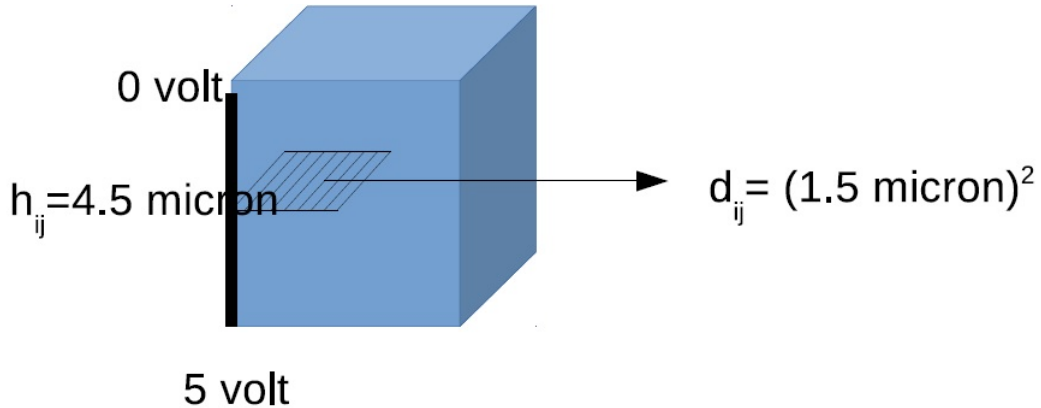


Figure 12: illustration of the dimensions of the pillar.

## 6 Testing the NLI for semiconductors

So far we have been dealing with linear materials, e.g. conductors and insulators. In order to test the interface for semiconductors, we start with replacing the metal in the test case (see Fig. 6) above with p-type and next n-type semiconductor. Using an homogeneous doping, we can mimic metallic behavior of a semiconducting pillar. We use a doping level of  $4.6 \times 10^{27} \text{ m}^{-3}$ . This gives an effective conductance of  $3330065.95604 \simeq 0.333 \times 10^7 \text{ S/m}$ , since  $\sigma_{effective} = q\mu_p p$  and  $p \simeq N_A$ . As before, we start with inspecting the Jacobian. The degrees of freedom are the following: In the central plane there are 4 nodes and each

node carries 3 degrees of freedom, being the Poisson potential, the hole fermi level and the electron fermi level. As before there are 8 vertical links carrying each 2 degrees of freedom, being the vector potential and the canonical momentum. Finally we add the contact voltages to the list to complete the set of field variables. There are 3 contacts participating. The degrees of freedom are ordered in the following way:

$$\{\psi_1, \psi_2, \psi_3, \psi_4, \phi_1^p, \phi_2^p, \phi_3^p, \phi_4^p, \phi_1^n, \phi_2^n, \phi_3^n, \phi_4^n, A_1, A_2, A_3, A_4, A_5, A_6, A_7, A_8, \Pi_1, \Pi_2, \Pi_3, \Pi_4, \Pi_5, \Pi_6, \Pi_7, \Pi_8, V_{C1}, V_{C2}, V_{C3}\}$$

As a consequence the  $\mathbf{x}$  vector has length 31. In order to understand the entries in the Jacobian, we show their grid locations in Fig. 13

In Fig. 14, we *translate the variables to indices* of the vector  $\mathbf{x}$ .

The Jacobian matrix of the first assembling sweep is listed below:

```
%%MatrixMarket matrix coordinate real general
% number of non-zeros: 122
%      row      col      value
31      31      186

----- Poisson part:

1      1      2.88647279946335e-07
1      2      -3.14766098997568e-16
1      3      -3.14766098997568e-16
1      5      -2.88647278799292e-07
1      9      -1.36411764218697e-30
1      21     4.70156957996368e-22
1      25     -4.70156957996368e-22
1      29     -1.04479323999193e-16
1      30     -1.04479323999193e-16
1      31     -3.10781717997599e-16
2      1      -3.14766098997568e-16
2      2      2.88647279946335e-07
2      4      -3.14766098997568e-16
2      6      -2.88647278799292e-07
2      10     -1.36411764218697e-30
2      22     4.70156957996368e-22
2      26     -4.70156957996368e-22
2      29     -1.04479323999193e-16
2      30     -1.04479323999193e-16
2      31     -3.10781717997599e-16
3      1      -3.14766098997568e-16
3      3      2.88647279946335e-07
3      4      -3.14766098997568e-16
3      7      -2.88647278799292e-07
```

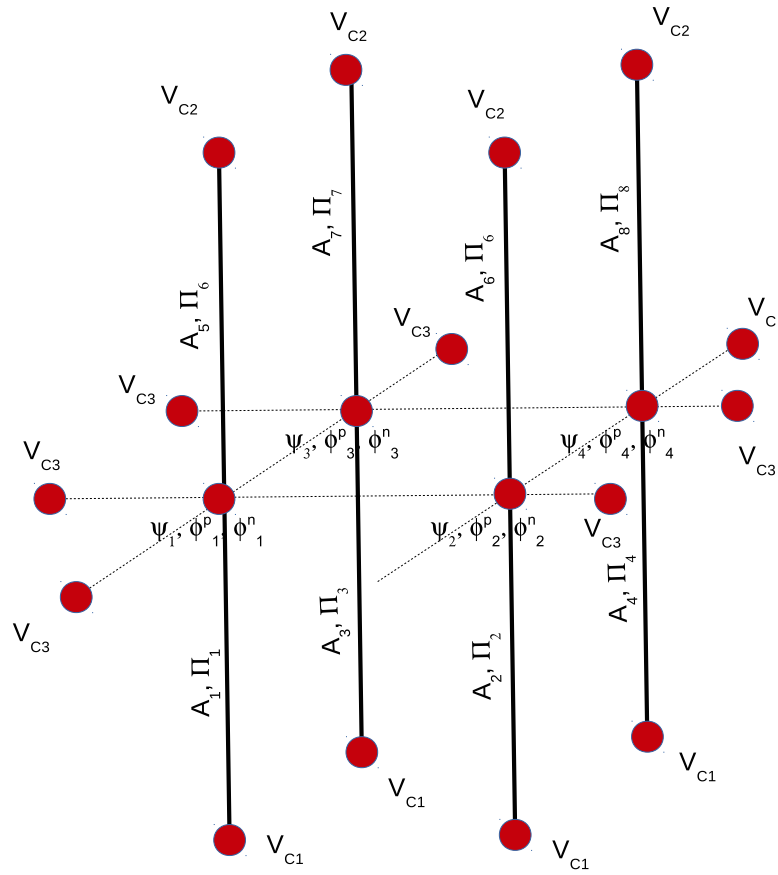


Figure 13: illustration of the variables location on the grid

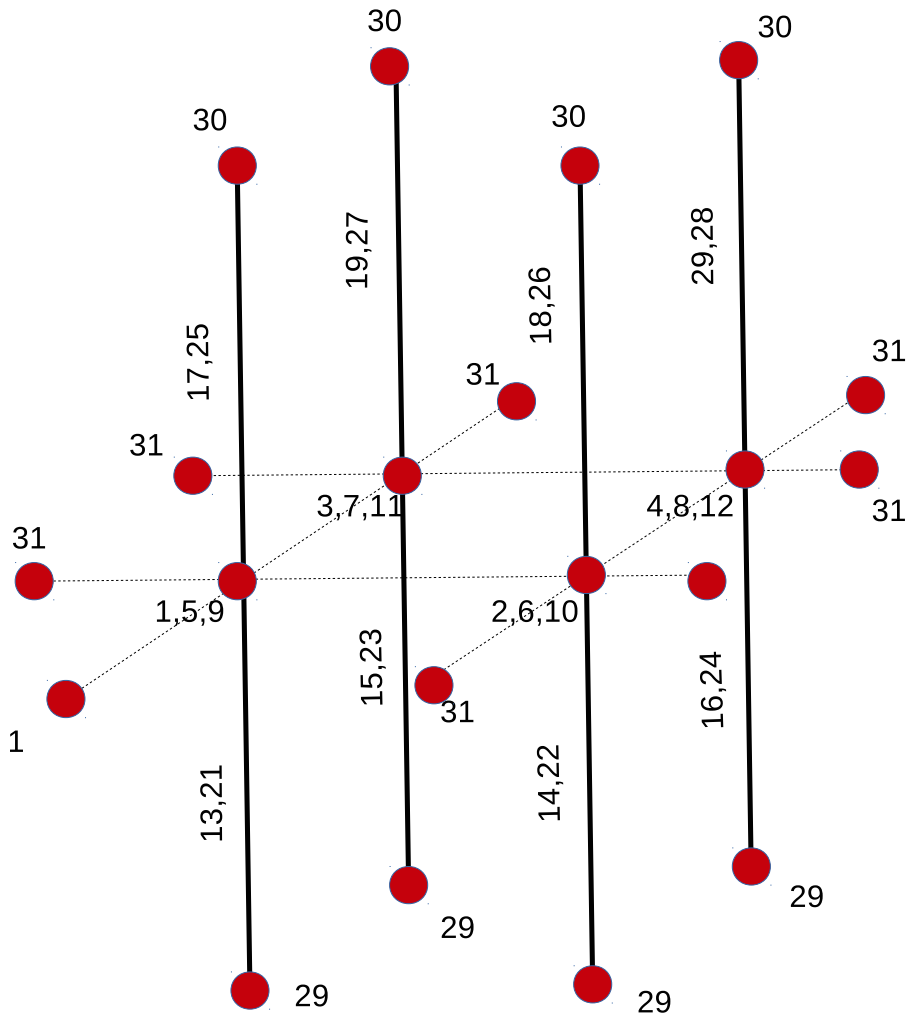


Figure 14: illustration of the variables indices on the grid

3	11	-1.36411764218697e-30
3	23	4.70156957996368e-22
3	27	-4.70156957996368e-22
3	29	-1.04479323999193e-16
3	30	-1.04479323999193e-16
3	31	-3.10781717997599e-16
4	2	-3.14766098997568e-16
4	3	-3.14766098997568e-16
4	4	2.88647279946335e-07
4	8	-2.88647278799292e-07
4	12	-1.36411764218697e-30
4	24	4.70156957996368e-22
4	28	-4.70156957996368e-22
4	29	-1.04479323999193e-16
4	30	-1.04479323999193e-16
4	31	-3.10781717997599e-16

----- FERMI part

5	1	-4.22149304866709e-06
5	5	4.46899304925902e-06
5	6	-1.0125e-07
5	7	-1.0125e-07
5	21	1.0125000015781e-13
5	25	-1.01250002505837e-13
5	29	-2.25000000350689e-08
5	30	-2.25000005568527e-08
6	2	-4.22149304866709e-06
6	5	-1.0125e-07
6	6	4.46899304925902e-06
6	8	-1.0125e-07
6	22	1.0125000015781e-13
6	26	-1.01250002505837e-13
6	29	-2.25000000350689e-08
6	30	-2.25000005568527e-08
7	3	-4.2214930486671e-06
7	5	-1.0125e-07
7	7	4.46899304925902e-06
7	8	-1.0125e-07
7	23	1.0125000015781e-13
7	27	-1.01250002505837e-13
7	29	-2.25000000350689e-08
7	30	-2.25000005568528e-08
8	4	-4.2214930486671e-06
8	6	-1.0125e-07
8	7	-1.0125e-07
8	8	4.46899304925902e-06
8	24	1.0125000015781e-13
8	28	-1.01250002505837e-13
8	29	-2.25000000350689e-08
8	30	-2.25000005568528e-08
9	1	1.46303092694563e-07
9	9	-9.71303090955283e-07
9	10	3.375e-07
9	11	3.375e-07
9	21	-3.37499992173242e-13
9	25	3.375e-13
9	29	7.49999982607204e-08
9	30	7.49999999999999e-08
10	2	1.46303092694563e-07
10	9	3.375e-07
10	10	-9.71303090955283e-07

10	12	3.375e-07
10	22	-3.37499992173242e-13
10	26	3.375e-13
10	29	7.49999982607204e-08
10	30	7.49999999999999e-08
11	3	1.46303092694563e-07
11	9	3.375e-07
11	11	-9.71303090955284e-07
11	12	3.375e-07
11	23	-3.37499992173242e-13
11	27	3.375e-13
11	29	7.49999982607205e-08
11	30	7.5e-08
12	4	1.46303092694563e-07
12	10	3.375e-07
12	11	3.375e-07
12	12	-9.71303090955284e-07
12	24	-3.37499992173242e-13
12	28	3.375e-13
12	29	7.49999982607205e-08
12	30	7.5e-08

----- A - Part :

13	21	-1
14	22	-1
15	23	-1
16	24	-1
17	25	-1
18	26	-1
19	27	-1
20	28	-1

----- Pi part :

21	1	7.46215317694971e-05
21	13	15.9154943091895
21	14	-3.58098621956764
21	15	-3.58098621956764
21	17	-1.59154943091895
21	21	3.35796892962737e-10
21	29	-7.46215317694971e-05
22	2	7.46215317694971e-05
22	13	-3.58098621956764
22	14	15.9154943091895
22	16	-3.58098621956764
22	18	-1.59154943091895
22	22	3.35796892962737e-10
22	29	-7.46215317694971e-05
23	3	7.46215317694973e-05
23	13	-3.58098621956764
23	15	15.9154943091895
23	16	-3.58098621956764
23	19	-1.59154943091895
23	23	3.35796892962738e-10
23	29	-7.46215317694973e-05
24	4	7.46215317694973e-05
24	14	-3.58098621956764
24	15	-3.58098621956764
24	16	15.9154943091895
24	20	-1.59154943091895
24	24	3.35796892962738e-10

24	29	-7.46215317694973e-05
25	1	-7.46215334999999e-05
25	13	-1.59154943091895
25	17	15.9154943091895
25	18	-3.58098621956764
25	19	-3.58098621956764
25	25	3.35796900749999e-10
25	30	7.46215334999999e-05
26	2	-7.46215334999999e-05
26	14	-1.59154943091895
26	17	-3.58098621956764
26	18	15.9154943091895
26	20	-3.58098621956764
26	26	3.35796900749999e-10
26	30	7.46215334999999e-05
27	3	-7.46215335e-05
27	15	-1.59154943091895
27	17	-3.58098621956764
27	19	15.9154943091895
27	20	-3.58098621956764
27	27	3.3579690075e-10
27	30	7.46215335e-05
28	4	-7.46215335e-05
28	16	-1.59154943091895
28	18	-3.58098621956764
28	19	-3.58098621956764
28	20	15.9154943091895
28	28	3.3579690075e-10
28	30	7.46215335e-05
29	1	48.9302996893657
29	2	48.9302996893657
29	3	48.9302996893658
29	4	48.9302996893658
29	21	-7.46215317694971e-05
29	22	-7.46215317694971e-05
29	23	-7.46215317694973e-05
29	24	-7.46215317694973e-05
29	29	-66.3302504617753
30	1	-16.582563
30	2	-16.582563
30	3	-16.582563
30	4	-16.582563
30	25	7.46215334999999e-05
30	26	7.46215334999999e-05
30	27	7.46215335e-05
30	28	7.46215335e-05
30	30	-66.3302519999999

Let us look into the details part after part. The first fragment

1	1	2.88647279946335e-07
1	2	-3.14766098997568e-16
1	3	-3.14766098997568e-16
1	5	-2.88647278799292e-07
1	9	-1.36411764218697e-30
1	21	4.70156957996368e-22
1	25	-4.70156957996368e-22
1	29	-1.04479323999193e-16
1	30	-1.04479323999193e-16
1	31	-3.10781717997599e-16

corresponds to the Poisson equation of  $V$  at node 1 (being the left-front node in the



semiconductor in the mid plane). (1,1) Is V-V self coupling. (1,2) and (1,4) are V-V neighbour couplings. (1,5) is  $V_1 - \phi_1^p$  coupling and (1,9) is  $V_1 - \phi_1^n$  coupling. All this corresponds to assembling of the Poisson equation. Furthermore there is a coupling to  $\Pi$  being (1,21) and (1,25). Finally there is a coupling to the 3 contacts, e.g. (1,29), (1,30) and (1,31). Now: are the values acceptable? Let is start with the off-diagonal element (1,2) is  $-3.14766098997568e-16$ . This element is composed from the Poisson equation. And the had calculation gives :  $-4.5 \times 1.5/3 \times 10^{-6} \times (11.9 + 3.9) \times 8.85418 \times 10^{-12}$  C/Nm =  $-3.1476 \times 10^{-16}$  C/V, which agrees with the reported values. The diagonal element is of this order plus a contribution from the charge density. The latter is  $q \times \Delta V \times \partial p/\partial V \simeq q \times \Delta V \times p = 1.602 \times 10^{-19} \times 4.5 \times 1.5 \times 1.5 \times 10^{-18} \times (-4.6) \times 10^{27} \times /0.02585 \times$  C/V =  $2.88648 \times 10^{-7}$  C/V. This is in agreement with the reported result is the NLI matrix. Now the matrix element (1,5) is expected to be of the same value. However the sign is flipped due to the derivative  $\partial p/\partial \phi^p = -\partial p/\partial \psi$ . The next element to inspect is (1,9). It is the derivative wrt  $\phi^n$ . Its numerical value is  $q \times \Delta V \times \partial n/\partial V \simeq q \times \Delta V \times p = 1.602 \times 10^{-19} \times 4.5 \times 1.5 \times 1.5 \times 10^{-18} \times (10^{16})^2/(4.6 \times 10^{27}) \times /0.02585 \times$  C/V =  $1.36407 \times 10^{-30}$  C/V. Again agreement is obtained. The element (1,21) is a  $V - \Pi$  coupling. Its-hand calculated value is  $\epsilon_0 \cdot (\epsilon_{oxid} \Delta A_{oxid} + \epsilon_{semi} \Delta A_{semi}) = -8.85418 \times 10^{-12} \times (3.9 + 3.9 + 3.9 + 11.9) \times 1.5 \times 1.5 \times 10^{-12} = 4.7015 \times 10^{-22}$  Cm/V. Thus the  $V - \Pi$  coupling is also properly extracted. Finally (1,29) , (1,30) and (1,31) are again  $V - V$  couplings and are of the same order of magnitude as (1,2) and (1,3).

Next we consider the Fermi part:

5	1	-4.22149304866709e-06
5	5	4.46899304925902e-06
5	6	-1.0125e-07
5	7	-1.0125e-07
5	21	1.0125000015781e-13
5	25	-1.01250002505837e-13
5	29	-2.25000000350689e-08
5	30	-2.25000005568527e-08

The elements (5,1) is a  $\phi^p - \psi$  coupling and (5,5) , (5,6) and (5,7) are  $\phi^p - \phi^p$  couplings. Elements (5,6) and (5,7) are off diagonal. There value is:  $\mu_p \times \Delta A dl_{ij} = 0.045 \times 2.25 \times 10^{-6}$  m<sup>3</sup>/sec =  $1.0125 \times 10^{-7}$  m<sup>3</sup>/sec. (We find also that the derivatives of the Bernoulli functions are  $-1/2$  for small values of the argument).

We have assembled the semi-conductor current continuity equations as

$$\left(\frac{1}{q}\right) \frac{\Delta(\text{vol})}{p} \left\{ \nabla \cdot \mathbf{J}_p + R + \frac{\partial p}{\partial t} \right\} = 0 \quad (57)$$

$$\left(\frac{1}{q}\right) \frac{\Delta(\text{vol})}{n} \left\{ -\nabla \cdot \mathbf{J}_n + R + \frac{\partial n}{\partial t} \right\} = 0 \quad (58)$$

Next consider the Pi part

21	1	7.46215317694971e-05
21	13	15.9154943091895
21	14	-3.58098621956764
21	15	-3.58098621956764
21	17	-1.59154943091895
21	21	3.35796892962737e-10
21	29	-7.46215317694971e-05

The element (21,13) is the  $Pi - A$  coupling and must be the same as the element (13,5) of the metallic case which indeed is the case. The element (21,1) seems of the same size as (13,1) in the metallic case.

## 7 Conclusion

In workpackage 1 of NANOCOPS has focused on two main subjects for providing field solving support for RF circuit simulation.

- A first major theme of work in WP1 has been to set up a 'holistic' co-simulation. The underlying idea is that circuits and fields each provide their own set of differential algebraic equations, and when correctly 'glued' together, i.e. giving a consistent and complete set of cross couplings, the newly assembled system is solvable.
- A second objective of the effort in WP1 was to support the tool development by applications to industrial-relevant cases and to arrive at a set of test cases serving as reference benchmarks. A series of cases have been presented both in D3.1 and the underlying deliverable. The effort not only deals with spatial discretization but also with time integration in circuit simulations and adaptive time stepping algorithms.

In order to achieve the goals an interface was constructed to couple an electromagnetic field solver and a circuit simulator in a holistic way by taking into account the coupling matrices of the field equations to the circuit variables. The technical realization is based on a master-slave process flow where the circuit simulator sends requests to the field solver to provide state updates of the field variables. The solving process requires the evaluation of the Jacobian, which was in a first implementation realized by evaluating numerical differentiation. This is prohibitively slow and therefore it was decided that the interface also should provide the Jacobian that is computed in the field solver at assembling stage. A major concern is the setting of the numerical language: when integrating two software tools at the level of pointer communication to data blocks, one should be aware of the dimensionality of these blocks, In the communication of the interface it is decided that all numbers that will be communicated are given in SI units. Once that the interface is operating properly based on these units, we may apply local and global scaling procedures. Much effort went into getting the scaling of the various parts in the Jacobian in place. A detailed reporting of the testing was done.

## References

- [1] S. Baumanns: *Coupled Electromagnetic Field/Circuit Simulation. Modeling and Numerical Analysis*. PhD thesis, University of Cologne, Logos Verlag Berlin, 2012.
- [2] S. Baumanns, L. Jansen, M. Selva-Soto, C. Tischendorf: *Analysis of semi-discretized differential algebraic equation from coupled circuit device simulation*. Computational and Applied Mathematics, Springer Basel, pp.1-23, 2014.
- [3] M. Hanke: *A New Implementation of a BDF method Within the Method of Lines*. Report No. 2001:01, Royal Institute of Technology, Stockholm, 2001.
- [4] D. Estevez Schwarz, C. Tischendorf: *Mathematical Problems in Circuit Simulation*, Mathematical Modelling of Systems, Vol. 1, 1996.

- [5] F. Mazzia, F. Iavernaro: *Test Set for Initial Value Problem Solvers, release 2.4*. Department of Mathematics, University of Bari, 2006. <http://pitagora.dm.uniba.it/~testset/>.
- [6] W. Schoenmaker, M. Matthes, B. De Smedt, S. Baumanns, C. Tischendorf, R. Janssen: *Large signal simulation of integrated inductors on semi-conducting substrates*. In Design, Automation Test in Europe Conference Exhibition (DATE), 2012, pages 1221-1226, 2012.
- [7] W. Schoenmaker, C. Tischendorf: *Jacobian Structure of Coupled Electromagnetic Field and Lumped Circuit Models*. Presentation at SCEE-2014 (Scientific Computing in Electrical Engineering), July 22, 2014, Wuppertal, Germany.
- [8] C. Strohm, C. Tischendorf: *Interface model integrating full-wave Maxwell simulation models into modified nodal equations for circuit simulation*. Presented in Minisymposium Mathematical Modeling for Nanoelectronic Coupled Problems at MATHMOD-2015, 8th Vienna International Conference on Mathematical Modelling, Feb. 20, 2015, Vienna, Austria.
- [9] K. Bittner, H.-G. Brachtendorf: *Fast algorithms for grid adaptation using non-uniform biorthogonal spline wavelets*, SIAM J. on Scientific Computing, to appear.